Langmuir

Article

pubs.acs.org/Langmuir

Fundamentals of Selective Ion Transport through Multilayer Polyelectrolyte Membranes

Chao Cheng,[†] Andriy Yaroshchuk,[‡] and Merlin L. Bruening*,[†]

[†]Department of Chemistry, Michigan State University, East Lansing, Michigan 48824, United States

[‡]ICREA and Department of Chemical Engineering, Polytechnic University of Catalonia, av. Diagonal 647, 08028 Barcelona, Spain

Supporting Information

ABSTRACT: Membranes composed of multilayer poly(4-styrenesulfonate) (PSS)/protonated poly(allylamine) (PAH) films on porous alumina supports exhibit high monovalent/divalent cation selectivities. Remarkably, the diffusion dialysis K^+/Mg^{2+} selectivity is >350. However, in nanofiltration this selectivity is only 16, suggesting some convective ion transport through film imperfections. Under $MgCl_2$ concentration gradients across either $(PSS/PAH)_4$- or $(PSS/PAH)_4PSS$-coated alumina, transmembrane potentials indicate Mg^{2+} transference numbers approaching 0. The low Mg^{2+} transference numbers with both polycation- and polyanion-terminated films likely stem from exclusion of Mg^{2+} due to its large size or hydration energy. However, these high anion/cation selectivities decrease as the solution ionic strength increases. In nanofiltration, the high asymmetry of membrane permeabilities to Mg^{2+} and Cl^- creates transmembrane diffusion potentials that lead to negative rejections (the ion concentration in the permeate is larger than in the feed) as low as −200% for trace monovalent cations such as K^+ and Cs^+. Moreover, rejection becomes more negative as the mobility of the trace cation increases. Knowledge of single-ion permeabilities is vital for predicting the performance of polyelectrolyte films in the separation and purification of mixed salts.

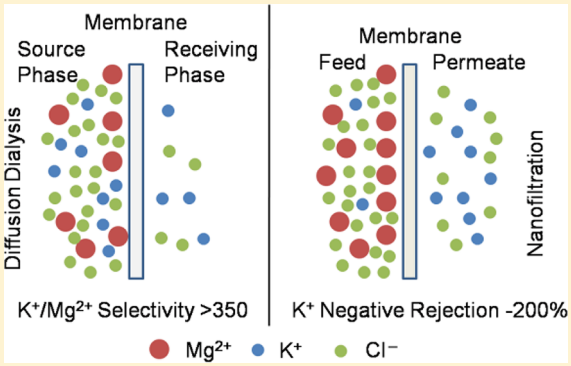

INTRODUCTION

Layer-by-layer adsorption of polycations and polyanions on porous supports is a convenient method for controlled formation of ultrathin membrane skins.[1,2] Although this multistep procedure may be cumbersome for large-scale membrane applications, polyelectrolyte multilayers (PEMs) on porous supports provide a unique platform for examining mechanisms of ion transport.[3,4] Commercial membranes, such as those formed by interfacial polymerization, are very effective in water treatment, but determining the properties of the membrane skin is challenging.[5−9] Deposition of PEMs on well-defined supports such as nanoporous alumina gives membrane skins whose thickness and surface charge controllably vary with the number of adsorbed layers. Transport properties also depend on the specific polyelectrolytes and the deposition conditions, i.e., pH and ionic strength.[10−14] Under optimized conditions, ultrathin PEMs can serve as the selective skins in pervaporation,[15−18] gas separation,[19,20] nanofiltration (NF),[21−24] and forward osmosis membranes.[25−28]

Similar to reverse osmosis (RO), NF involves pressure-driven passage of water or another solvent through a membrane. However, RO membranes are denser than NF membranes, so NF requires lower pressures for a given flux, and monovalent ion rejections are typically lower in NF than RO. The solution-diffusion model,[29] which assumes that transport through the membrane occurs solely by diffusion, adequately describes RO, but NF membranes may contain pores large enough to allow for some convective salt transport.[30,31] Supported PEMs behave as NF membranes, selectively rejecting divalent ions.[21,23] Moreover, the well-defined structure of PEMs gives a convenient system to examine the applicability of the solution-diffusion model through a combination of NF experiments and diffusion dialysis.

Tieke and co-workers first reported Na^+/Mg^{2+} diffusion dialysis selectivities as high as 113 with 60-bilayer protonated poly(allylamine) (PAH)/poly(4-styrenesulfonate) (PSS) films on a porous polymer support. Films with 5 and 10 bilayers showed selectivities between 30 and 40.[14] In later dead-end, single-salt NF experiments, the Na^+/Mg^{2+} selectivity was only 10 for 0.01 M chloride salt solutions, even with a 60-bilayer polyvinylamine/poly(vinyl sulfate) film. Nevertheless, selectivities appeared to be higher at lower salt concentrations (0.001 M) where Mg^{2+} rejections approached 100%.[32] Ouyang and co-workers achieved 95% Mg^{2+} rejection along with a Na^+/Mg^{2+} selectivity of 22 using feed solutions containing both NaCl and $MgCl_2$ and porous alumina membranes coated with $(PSS/PAH)_5$ films.[21] However, they presented no diffusion dialysis studies, so testing of the solution-diffusion model was not possible.

Received: November 15, 2012
Revised: January 9, 2013
Published: January 14, 2013

In addition to simple diffusion, electric fields that arise spontaneously due to different membrane permeabilities to cations and anions also influence ion transport across NF and RO membranes. This is especially evident in NF of mixed salt solutions, where the concentration of a given ion may be higher in the permeate than in the feed (negative rejection).[21,33,34] In particular with solutions containing both NaCl and $MgCl_2$, NF through $(PSS/PAH)_4$ membranes results in small negative Na^+ rejections (about −30%)[21] because the PEMs are more permeable to Cl^- and Na^+ than Mg^{2+}.[14] Initial passage of excess Cl^- creates a negative potential that pulls extra Na^+ through the membrane (see Figure 1).

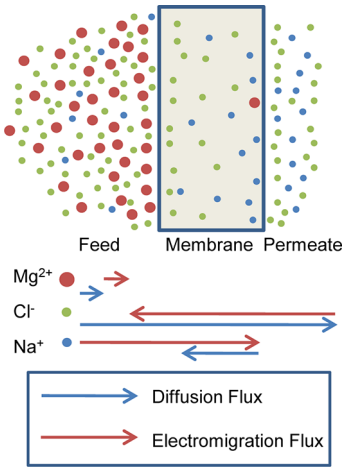

Figure 1. Schematic, qualitative drawing of ion distributions and transport during NF of a solution containing $MgCl_2$ and trace amounts of NaCl. The high permeability of Cl^- relative to Mg^{2+} leads to a negative electric potential drop across the membrane. This potential enhances the transport of trace Na^+ ions and can lead to higher concentrations of Na^+ in the permeate than in the feed. The arrows qualitatively show the relative fluxes due to diffusion (blue) and electromigration (red) for each ion. In the absence of convection, the total flux is the sum of the arrows.

This study examines the mechanisms of cation transport through PEMs deposited on nanoporous alumina. Specifically, we first combine diffusion dialysis and NF experiments to determine whether the solution-diffusion model applies to NF through PEMs. Second, we measure transmembrane potentials to investigate the selectivity of the PEMs for anions over cations at various salt concentrations. These studies also include an examination of diffusion dialysis and NF as a function of salt concentrations. Finally, we study negative rejections of trace ions, which depend on both the electric potential developed across the membrane (due to anion/cation selectivity) and the membrane permeability to the trace ions.

EXPERIMENTAL SECTION

Materials. Poly(sodium 4-styrenesulfonate) (M_w = 70 000 Da) and poly(allylamine hydrochloride) (M_w = 15 000 Da) were obtained from Aldrich. Salts were purchased from Columbus Chemical with the exception of CsCl (Aldrich) and LiCl (Jade Scientific). LiCl and CsCl are hygroscopic, so we prepared stock solutions from freshly opened bottles. All chemicals were used as received without further purification. Deionized water (Milli-Q system, 18.2 MΩ·cm) was employed in all experiments. The pH of the polyelectrolyte solutions was adjusted with dilute aqueous HCl or NaOH.

Film Deposition. Porous alumina membranes (0.02 μm Whatman Anodisk filters, all membranes were used from the same box unless specified otherwise) were treated with UV/O_3 (Boekel UV-Clean Model 135500) for 15 min and placed in a home-built O-ring holder that exposes only the feed side of the membrane to polyelectrolyte solutions. The deposition solutions (pH 2.3) contained 0.02 M (with respect to the repeating unit) polyelectrolytes along with 1 M NaCl for PAH and 0.5 M NaCl for PSS. The low deposition pH is common for PSS/PAH films,[35] and addition of 1 M NaCl to PAH adsorption solutions leads to a high surface charge for monovalent/multivalent ion separations.[21] Polyelectrolyte multilayers were adsorbed by alternatively exposing the top surface of the membrane to polyanion and polycation solutions for 5 min with 1 min rinsing with deionized water between each deposition step. PEMs usually contained four PSS/PAH bilayers to allow high water flux while still providing full coverage of the support.[11,21]

Nanofiltration. NF experiments were performed with a home-built system described previously.[22] Briefly, the crossflow apparatus was pressurized with N_2, and a centrifugal pump circulated the feed solution across the membranes at 26 mL/min to minimize concentration polarization. A stainless steel prefilter (Mott Corp.) removes rust or insoluble particles prior to passing solution over the membrane. The exposed membrane external area was 1.7 cm^2. After 18 h of filtration to reach steady state, permeate aliquots (<10 mL) were collected for periods ranging from 30 min to 2 h, and the feed solution was sampled at the end of the experiment. The feed volume was initially 2 L. The concentrations of most cations were determined using inductively couple plasma-optical emission spectroscopy (Varian 710-ES). Cs^+ was analyzed by atomic emission spectroscopy (Varian AA240), and nitrobenzene was analyzed by UV−vis absorbance measurements (PerkinElmer Lambda 40). The rejection, *Re*, was calculated with eq 1, where C_f and C_p are the feed and permeate concentrations, respectively. Selectivity, for ion 1 over ion 2, $\alpha_{1/2}$, was calculated using eq 2.

$$Re = \frac{C_f - C_p}{C_f} \tag{1}$$

$$\alpha_{1/2} = \frac{C_{1,p}/C_{1,f}}{C_{2,p}/C_{2,f}} = \frac{1 - Re_1}{1 - Re_2} \tag{2}$$

Multiple permeate samples from each of at least two membranes were collected for determination of ion rejections and solution fluxes. The ± values represent standard deviations of at least four values.

Diffusion Dialysis. Diffusion dialysis was performed as described previously.[36] A membrane was sandwiched between the source and receiving cells, and the solutions in each cell (initially 90 mL each) were stirred vigorously. The cells exposed a membrane area of 2.1 cm^2. 1 mL aliquots were withdrawn periodically from the receiving cell to monitor the analyte concentration as a function of time, and similar aliquots were taken from the source phase to maintain equal volumes. Because the diffusion flux is relatively small, the concentration gradient across the membrane is essentially constant. Moreover, the transporting salt concentration in the source phase was limited to 0.01 M to minimize osmosis. In most experiments, the receiving phase was initially deionized water. For diffusion dialysis experiments as a function of solution composition, we added a background salt in equal concentrations to both the source and receiving reservoirs to keep osmosis and diffusion of the added salt negligible. At least three membranes were used to obtain the diffusion fluxes, and ± values represent standard deviations where *n* is typically 3.

Membrane Potential. Membrane potential measurements were carried out using the diffusion dialysis apparatus (no convective flow) with solutions containing different salt concentrations on each side of the membrane. Before measuring the transmembrane potential, the two Ag/AgCl reference electrodes (saturated KCl, CH Instruments) were placed in the receiving phase solution to determine the electric potential difference between these electrodes. This potential drop was subtracted from the membrane potential reading, which was obtained when the reference electrodes were placed on the different sides of the membrane. The difference between the junction potentials of the electrodes in the source and receiving solutions was also subtracted

dx.doi.org/10.1021/la304574e | Langmuir 2013, 29, 1885−1892

(see the Supporting Information). To minimize the diffusion boundary layers at the membrane surface, both solutions were stirred vigorously. Solution activity coefficients for KCl,[37,38] $MgSO_4$,[39] and $MgCl_2$[40] were usually obtained by interpolation of literature data. For $MgCl_2$ at concentrations ≤0.004 64 M, activity coefficients were estimated from the Debye–Hückel equation. Three membranes were used to obtain values of the membrane potential, and ± values represent standard deviations.

RESULTS AND DISCUSSION

Ion transport through PEMs may include diffusion, convection, and electromigration components, and the film permeability often varies with the solution composition.[41] Thus, ion flux is a complicated function of salt concentrations and transmembrane volume flow. To evaluate the effects of different variables on transport, this section first examines salt permeabilities in diffusion dialysis where transmembrane volume flow is negligible. Subsequent NF studies show that transmembrane volume flow significantly enhances ion transport, and measurements of membrane potentials assess relative permeabilities of cations and anions. Finally, NF measurements with mixed salts at varying concentrations show remarkable negative rejections due to spontaneously arising transmembrane electric potentials that result from higher membrane permeabilities to anions than cations.

Diffusion Dialysis. In dialysis experiments, ions diffuse across a membrane from a concentrated source phase to a dilute receiving phase. Figure 2 shows the evolution of the amounts of K^+ and Mg^{2+} in the receiving phase during aqueous dialysis of 0.01 M $MgCl_2$ or 0.01 M KCl through a porous alumina membrane coated with a $(PSS/PAH)_4$ film. (The receiving phase initially contains deionized water.) Based on the slopes in Figure 2 and in similar replicate experiments, the flux of KCl is $(2.4 \pm 0.5) \times 10^{-9}$ mol cm^{-2} s^{-1}, whereas the flux of $MgCl_2$ is $<7 \times 10^{-12}$ mol cm^{-2} s^{-1}. As Table 1 shows, these fluxes lead to a remarkable K^+/Mg^{2+} selectivity >350, and in dialysis with a source phase solution containing both $MgCl_2$ and KCl, the fluxes of each cation are essentially similar to those in single-salt experiments. Tieke and co-workers performed dialysis using $(PSS/PAH)_{60}$ films on porous poly(acrylonitrile)/poly(ethylene terephthalate) supports and achieved a Na^+/Mg^+ selectivity of 113 with source phase concentrations of 0.1 M.[14] The support and number of layers in the film as well as the source phase concentration likely affect selectivities.

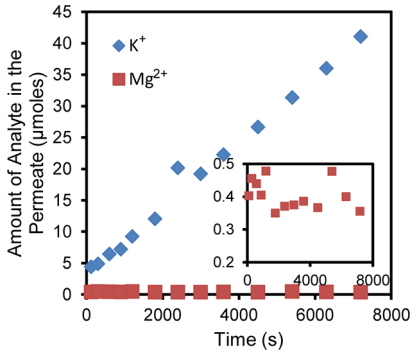

Figure 2. Amount of KCl (blue diamonds) or $MgCl_2$ (red squares) in the receiving phase as a function of time in diffusion dialysis of 0.01 M KCl or 0.01 M $MgCl_2$ through a porous alumina membrane coated with a $(PSS/PAH)_4$ film. The inset shows an enlarged region for the $MgCl_2$.

Table 1. Ion Fluxes and Selectivities in Diffusion Dialysis of KCl and $MgCl_2$ through Bare Porous Alumina Membranes and Similar Membranes Coated with $(PSS/PAH)_4$ and $(PSS/PAH)_4PSS$ Films

membrane	ion	single salt ion flux (nmol cm^{-2} s^{-1})	selectivity (K^+/Mg^{2+})
bare alumina	K^+	6.43 ± 0.65	1.47 ± 0.15
	Mg^{2+}	4.36 ± 0.04	
$(PSS/PAH)_4$-coated alumina	K^+	2.39 ± 0.50	>350
	Mg^{2+}	<0.007	
$(PSS/PAH)_4PSS$-coated alumina	K^+	3.09 ± 0.18	276 ± 93
	Mg^{2+}	0.011 ± 0.004	

Dialysis using porous alumina coated with a $(PSS/PAH)_4PSS$ film gives salt fluxes (Table 1) similar to those with $(PSS/PAH)_4$-coated membranes. Hence, the surface charge is not a dominant factor in controlling transport, and the K^+/Mg^{2+} selectivity likely results primarily from the difference in hydrated ion sizes (or solvation energies) rather than charge exclusion. Previous SEM images of these membranes show that the interiors of the pores are open, and selectivity only increases dramatically after full coverage of the support.[11,21] Thus, the primary effect of the polyelectrolyte adsorption results from the film on the surface and not adsorption within pores.[42] The relatively dense PEM structure is essentially impermeable to Mg^{2+} (hydrated diameter of 8 Å) but much more permeable to K^+ (hydrated diameter of 3 Å).[43] Studies with the transport of neutral molecules suggest that the effective pore diameter in $(PSS/PAH)_7$ films is around 0.8–1.0 nm, which is consistent with the exclusion of Mg^{2+}.[36]

Ion fluxes through these composite membranes are affected by both the PEM and the alumina support. In each of these membrane regions, eq 3 describes the salt flux, J, where ΔC is the concentration gradient across the region and P is the local permeance.

$$J = P\Delta C \tag{3}$$

According to the series resistance model,[44] eq 4 describes the permeance of the PEM, P_{film}, where $P_{composite}$ is the permeance of the PEM-coated membrane and

$$P_{film} = \frac{P_{composite}P_{support}}{P_{support} - P_{composite}} \tag{4}$$

$P_{support}$ is the permeance of the bare alumina. We calculated the values of $P_{composite}$ and $P_{support}$ for KCl using eq 3 with 0.01 M for ΔC and diffusion fluxes of 6.4 and 2.4 nmol cm^{-2} s^{-1} through the bare and modified membranes, respectively. Equation 4 then reveals that the permeance of the PEM, P_{film}, is 3.8 μm/s. In contrast, the PEM permeance to $MgCl_2$ is <0.007 μm/s.

Nanofiltration. In NF with PEM-coated porous alumina, a pressure drop forces water across the membrane while the feed solution flows parallel (crossflow) to the membrane surface. If water and ion transport occur solely by independent diffusion, the solution-diffusion model should describe the ion rejection. In this model, eq 3 still describes the salt flux across the membrane, with $P = P_{film}$. Assuming negligible concentration polarization in the feed solution, or $\Delta C_{film} = C_f - C_p$, eq 5

dx.doi.org/10.1021/la304574e | Langmuir 2013, 29, 1885–1892

Table 2. Experimental and Predicted Ion Rejections and K^+/Mg^{2+} Selectivities in NF[a] of 0.01 M KCl or 0.01 M $MgCl_2$ through Porous Alumina Membranes Coated with $(PSS/PAH)_4$ Films

predicted values[b]			experimental values				
rejection (%)			rejection (%)		solution flux ($m^3/(m^2$ day))		
K^+	Mg^{2+}	selectivity (K^+/Mg^{2+})	K^+	Mg^{2+}	K^+	Mg^{2+}	selectivity (K^+/Mg^{2+})
85.3 ± 4.27	>99.96	>350	47.3 ± 4.4	96.7 ± 0.7	1.91 ± 0.07	1.61 ± 0.07	16.0 ± 1.3

[a]NF occurred with a transmembrane pressure of 5 bar and a crossflow rate of 26 mL/min. [b]The predicted values were calculated from the diffusion dialysis results and the solution-diffusion model.

describes the salt rejection based on the solution-diffusion model

$$Re = 1 - \frac{P_{film}}{J_v + P_{film}} \quad (5)$$

where J_v is the volumetric flux through the membrane (see the Supporting Information for more details on the solution-diffusion model).

Table 2 shows experimental and predicted salt rejections in NF with alumina membranes coated with $(PSS/PAH)_4$ films. We predicted the rejections using the P_{film} values from diffusion dialysis, the experimental values of J_v, and eq 5. Notably, the solution-diffusion model greatly overpredicts the NF rejections. Although the K^+/Mg^{2+} selectivity in NF is 16, which is similar to the Na^+/Mg^{2+} selectivity in our previous work,[21] this selectivity is much lower than the value of >350 observed in diffusion dialysis.

The lower than expected rejections in NF likely stem from convective transport of ions. However, given the assumption of a ~20 nm[21] thick polyelectrolyte layer, the permeability coefficients estimated from the diffusion dialysis data are 4 and 7 orders of magnitude lower than the bulk diffusivities for KCl and $MgCl_2$, respectively. Such strongly reduced diffusivities are hardly compatible with the picture of a nanoporous medium, which is required to have noticeable convective coupling in a defect-free matrix. Thus, the increased passage of $MgCl_2$ in NF most likely stems from convection through film imperfections that arise due to inhomogeneities in the alumina support. Some SEM images reveal defects in the alumina skin layer on the porous alumina supports (see Supporting Information Figure S5), and such imperfections will likely lead to defects in the PEM. NF rejections and diffusion dialysis fluxes seem to vary when we use membranes taken from different boxes, and SEM images suggest that the defect density varies from box to box (see the Supporting Information). Therefore, the data above were all obtained using one box of alumina supports.

Concentration polarization may also decrease K^+/Mg^{2+} selectivity in NF compared to diffusion dialysis. However, the Mg^{2+} rejection is not a strong function of either crossflow rate or permeate flux, so concentration polarization is not the primary factor leading to low rejection. Moreover the concentration polarization factors needed to make the NF results consistent with dialysis data seem unreasonably high (see section 4 of the Supporting Information for a longer discussion of concentration polarization).

Membrane Potential. The rate of salt diffusion through a membrane depends on the solubility and diffusivity of both the cation and the anion, but transport experiments typically assess only a composite salt permeance. In contrast, electrical potential drops across membranes exposed to salt concentration gradients inherently reveal the relative permeabilities of cations and anions. Ideally, the electrical potential drop across the membrane, E, is a function of the transference numbers of the cation and anion, t_+ and t_-, respectively, according to eq 6.[45]

$$E = \left(\frac{t_+}{z_+} + \frac{t_-}{z_-}\right)\frac{RT}{F}\ln\left(\frac{a_1}{a_2}\right) \quad (6)$$

In this equation, R is the gas constant, z_+ and z_- represent the charges of the cation and anion, respectively, T is the temperature, F is the Faraday constant, and a_1 and a_2 are the salt activities in the source and receiving phase solutions, respectively. The transference numbers depend on the charge, concentration, and diffusivity of each ion, as eq 7 shows for the cation.

$$t_+ = \frac{|z_+|C_+D_+}{|z_+|C_+D_+ + |z_-|C_-D_-} \quad (7)$$

In this equation, C_+ and C_- are the concentrations and D_+ and D_- are the diffusion coefficients of the cation and anion, respectively. Because for $MgCl_2$ most of the mass transport resistance of the coated membrane stems from the PEM, the transference number is essentially that in the film, and the support can be neglected. For KCl, the transference number reflects the selectivity of both the support and the PEM.

Figure 3 shows the potential drop across $(PSS/PAH)_4$- and $(PSS/PAH)_4PSS$-coated alumina membranes as a function of

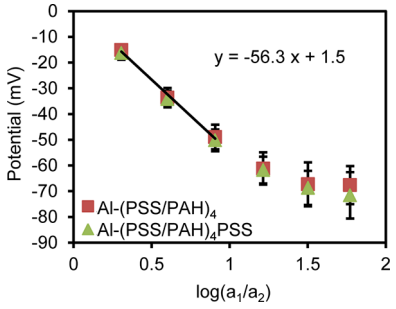

Figure 3. Transmembrane potential as a function of $\log(a_1/a_2)$, where a_1 and a_2 are the activities of $MgCl_2$ in the source and receiving phases, respectively. The source phase $MgCl_2$ concentrations ranged from 0.001 to 0.0215 M, whereas the receiving phase always contained 0.001 M $MgCl_2$. Squares and triangles represent alumina membranes coated with $(PSS/PAH)_4$ and $(PSS/PAH)_4PSS$ films, respectively.

$\log(a_1/a_2)$ for $MgCl_2$ solutions. (In these experiments, the receiving phase concentration is always 0.001 M.) For low source phase concentrations, the slopes of the linear fits to data for both types of membranes are around −57 mV, indicating that the transference number for Mg^{2+} is essentially zero. For completely selective membranes with no permeability to Mg^{2+}, the slope would be −59 mV. The low Mg^{2+} transference

dx.doi.org/10.1021/la304574e | Langmuir 2013, 29, 1885−1892

number is consistent with the negligible $MgCl_2$ flux in diffusion dialysis. Regardless of whether the film terminates with PAH or PSS, the membrane is much less permeable to Mg^{2+} than Cl^-, suggesting that size exclusion or a difference in ion solvation energies is the dominant mechanism behind the low Mg^{2+} transference number. The high electric field across the PEM (as high as 35 000 V/cm) is common in interfaces and double layers.[45]

At the higher source phase concentrations in Figure 3, the decrease in slope implies that the Mg^{2+} transference number increases with the $MgCl_2$ concentration. Fixing the source to receiving phase concentration ratio at 2 while varying the concentrations in both solutions more clearly reveals the influence of ionic strength on transference number. As Figure 4a shows, the Mg^{2+} transference number increases from around 0 with a 0.0043 M $MgCl_2$ source phase to 0.42 in a 0.20 M $MgCl_2$ source phase. This trend occurs with both $(PSS/PAH)_4$ and $(PSS/PAH)_4PSS$ films, suggesting that the increasing transference number at high ionic strength is not simply due to screening of surface charge and that the membrane becomes more permeable to Mg^{2+} as the $MgCl_2$ concentrations increases. Farhat and Schlenoff provided evidence that at high ionic strength polycations and polyanions dissociate to create more ion-exchange sites and enhance transport.[41] Control experiments with uncoated porous alumina also show more permeability to Cl^- than Mg^{2+}, presumably because the alumina is positively charged. However, the effect is much smaller than in coated membranes (Figure 4a). At the lowest concentrations, the potential drops across bare membranes are only −8.3 mV compared to −16.7 mV across membranes coated with $(PSS/PAH)_4$ films.

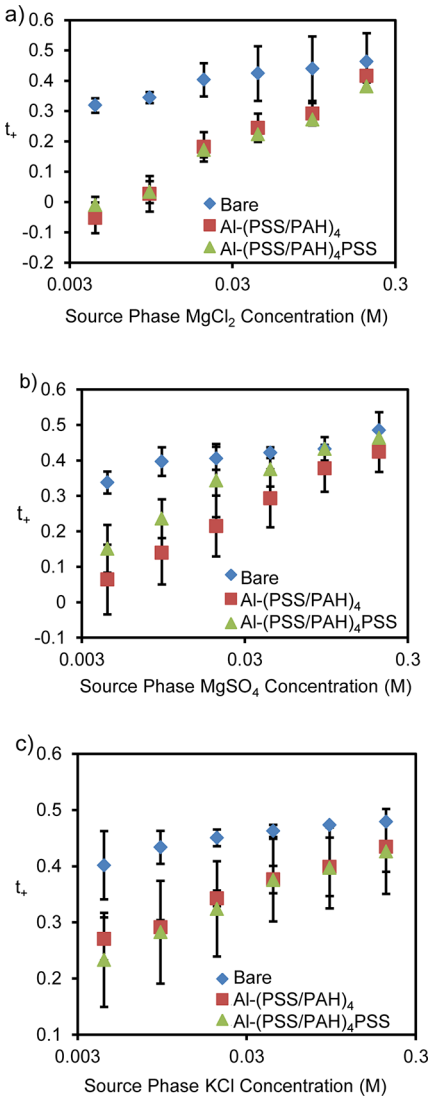

Figure 4. Transference numbers of cations as a logarithmic function of the (a) $MgCl_2$, (b) $MgSO_4$, and (c) KCl source phase concentrations (from 0.0043 to 0.20 M) employed in transmembrane potential measurements with bare alumina membranes (diamonds), $(PSS/PAH)_4$-coated membranes (squares), and $(PSS/PAH)_4PSS$-coated membranes (triangles). The ratios of the source and receiving phase concentrations are 2 in all cases.

Despite the large size of SO_4^{2-} relative to Cl^-, the Mg^{2+} transference numbers for $MgSO_4$ diffusion through $(PSS/PAH)_4$-coated membranes are only slightly smaller than those with $MgCl_2$ (compare Figures 4a and 4b). The Mg^{2+} transference number is <0.1 with 0.0043 M $MgSO_4$ in the source phase (Figure 4b). PSS-terminated membranes likely electrostatically exclude SO_4^{2-},[23] and this might explain why in the case of $MgSO_4$ the Mg^{2+} transference numbers are a little higher for $(PSS/PAH)_4PSS$ films than $(PSS/PAH)_4$ films.

Interestingly, at source phase concentrations of 0.0043 M, even KCl shows a cation transference number of only ∼0.25 (Figure 4c). This is in contrast to aqueous solutions where the potassium and chloride transference numbers are nearly equal.[45] The low cation transference number stems in part from the positively charged alumina substrate, which excludes cations, but the K^+ transference number is significantly lower for membranes coated with $(PSS/PAH)_4$ and $(PSS/PAH)_4PSS$ than for bare alumina. The low K^+ transference number suggests a slight positive charge on these films.[46]

Diffusion Dialysis and Nanofiltration as a Function of Solution Composition. The transmembrane potential measurements suggest that the membrane permeability to Mg^{2+} increases with the ionic strength of the surrounding solution. To further assess the effect of ionic strength on ion transport, we performed diffusion dialysis of 0.01 M KCl while adding equal amounts of $MgCl_2$ to the source and receiving reservoirs. Figure 5 shows that on going from 0 to 0.0464 M $MgCl_2$ in both the source and receiving phases the K^+ flux

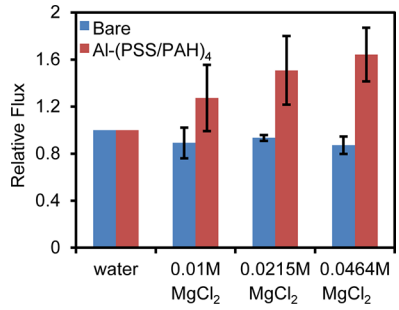

Figure 5. Normalized K^+ fluxes in diffusion dialysis of 0.01 M KCl through bare and $(PSS/PAH)_4$-coated alumina membranes. All experiments occurred with 0.01 M KCl as the source phase, and the $MgCl_2$ concentrations in the source and receiving phases varied simultaneously from 0 to 0.0464 M. Fluxes are normalized to those with no $MgCl_2$, which were 6.4 and 2.4 nmol cm^{-2} s^{-1} for bare and coated membranes, respectively. (All experiments with diffusion dialysis as a function of salt composition were performed using alumina supports from a new box.)

dx.doi.org/10.1021/la304574e | Langmuir 2013, 29, 1885−1892

increases by a factor of ~1.6. The corresponding addition of $MgCl_2$ to both source and receiving phases in diffusion dialysis with bare alumina does not increase flux. Thus, the primary effect of $MgCl_2$ addition is an increase in the permeability of the polyelectrolyte film to KCl. Similarly, the Mg^{2+} permeability (0.01 M $MgCl_2$ in the source phase) increases ~1.5 times upon the addition of 0.119 M KCl to both source and receiving phases. (The addition of 0.119 M KCl gives the same solution ionic strength as the addition of 0.0464 M $MgCl_2$ to 0.01 M KCl.)

Compared to diffusion dialysis, NF may show different trends in ion flux as a function of ionic strength because ion transport occurs in part through convective coupling with water flux. As Figure 6a shows, within experimental uncertainty, the

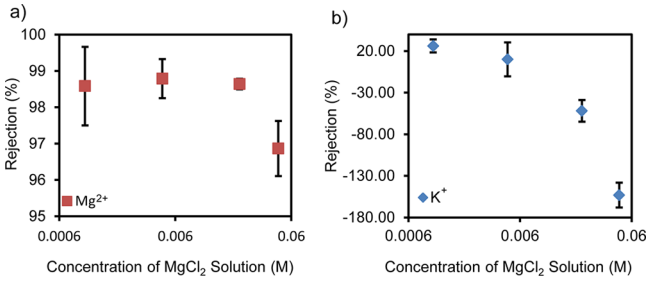

Figure 6. Rejections of (a) $MgCl_2$ and (b) trace KCl in NF through porous alumina membranes coated with $(PSS/PAH)_4$ films. The $MgCl_2$ feed concentrations ranged from 0.0010 to 0.0464 M while the KCl concentration was 0.5% of that for $MgCl_2$. Both graphs are from the same experiments repeated with more than three membranes. The applied pressure was adjusted from 2.8 to 6 bar to keep the difference between the applied pressure and osmotic pressure approximately the same and maintain a nearly constant volume flux. The crossflow rate was 26 mL/min.

$MgCl_2$ rejection in NF is constant with feed concentrations ranging from 0.001 to 0.0232 M $MgCl_2$ (rejection ranged from 98.6 to 98.8%). At an even higher feed concentration (0.0464 M), the rejection decreases slightly to 96.9%. The results in Figure 6a are mostly consistent with a primary Mg^{2+} transport mechanism of convective coupling, probably through defects. In transport through defects the Mg^{2+} flux should be proportional to the $MgCl_2$ feed concentration, and rejection should be independent of concentration.

Negative Rejections in Nanofiltration. Diffusion potentials created by $MgCl_2$ transport through imperfection-free regions of the membrane may affect the transport of other charged species. This should be particularly true for K^+ because diffusion through the defect-free region may dominate its transport. To examine the effects of $MgCl_2$ on the transport of other species in NF, we added trace amounts of nitrobenzene (0.10 mM) and KCl (0.5% of the concentration of $MgCl_2$) to the NF solutions. The nitrobenzene rejection is ~20%, regardless of $MgCl_2$ concentration, suggesting that the presence of $MgCl_2$ has a marginal effect on the overall membrane permeability. Consistent with minimal variation in film permeability to nitrobenzene, the water flux is also relatively constant at essentially equal driving pressures. We varied the applied pressure to keep the driving force, applied pressure minus osmotic pressure, for solution flux approximately constant, and the solution flux ranged from 0.63 to 0.86 $m^3/(m^2\ day)$ over the range of $MgCl_2$ feed concentrations in Figure 6.

In contrast to $MgCl_2$, Figure 6b shows that NF rejection of K^+ decreases significantly with increasing $MgCl_2$ concentrations and becomes highly negative. At the highest Mg^{2+} feed concentration, the amount of K^+ in the permeate is 2.5 times that in the feed. The negative rejection reflects a negative electrical potential drop (from feed to permeate) across the membrane that enhances K^+ and Mg^{2+} transport while decreasing transport of Cl^- to maintain zero current (see Figure 1). However, the reason for the decreasing K^+ rejection with increasing $MgCl_2$ concentration is not readily evident because the transference numbers obtained from membrane potentials decrease with increasing $MgCl_2$ concentration (see Figure 4a). Increased permeability to K^+ with increasing $MgCl_2$ concentrations (Figure 5) can compensate a fraction of the decreased membrane potentials at higher $MgCl_2$ concentrations, but this may not account for the 3-fold increase in K^+ passage on going from 0.0010 to 0.0464 M $MgCl_2$ as the dominant salt.

The high negative rejections might stem from selective convective transport of Cl^- over Mg^{2+} in the defect-free region of the matrix. Such a mechanism should increase transmembrane potentials and give more negative rejections with increases in permeate flux. However, Figure 7 clearly shows less

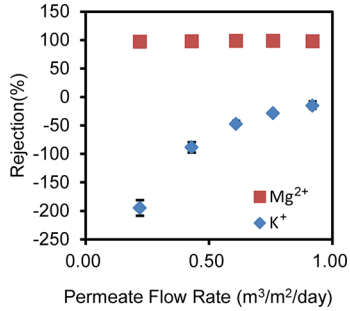

Figure 7. $MgCl_2$ and KCl rejections as a function of permeate flow rate in NF of 0.0215 M $MgCl_2$, 0.11 mM KCl through porous alumina coated with a $(PSS/PAH)_4$ film. The Mg^{2+} rejections range from 97.1% to 98.7%. The applied pressure varied from 2 to 5 bar, and the crossflow rate was 26 mL/min. (Figure S4 shows an enlarged plot of the Mg^{2+} rejection.)

negative K^+ rejection as flux increases. In fact, the concentration of K^+ in the permeate is almost proportional to the solution flux. This shows that K^+ flux, which predominantly occurs through diffusion and electrical migration, is essentially independent of solution flux, and higher permeate flow rates simply dilute the K^+. Thus, selective convective transport of Cl^- over Mg^{2+} does not contribute to negative rejection. Currently, we do not have a satisfactory explanation for why the K^+ NF rejection becomes more negative with increasing concentrations of $MgCl_2$, although increases in film permeability may contribute to this phenomenon. The Mg^{2+} rejection is relatively independent of solution flux (see Figure 7 and Figure S4), so for this highly rejected ion, convective coupling (presumably mostly through defects) is important because diffusion through the membrane is very slow.

Consistent with negative rejection stemming from electrical migration, the trace cation rejection varies with the mobility of the cation. Figure 8a shows rejections of trace Li^+, K^+, and Cs^+. The mobility of Li^+ is about half that of K^+ and Cs^+, and the amount of Li^+ passing through the membrane is indeed about

dx.doi.org/10.1021/la304574e | Langmuir 2013, 29, 1885−1892

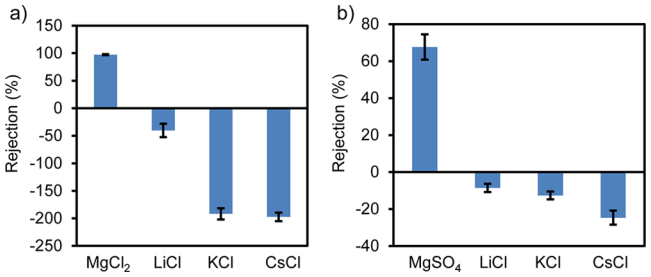

Figure 8. Ion rejections during NF of solutions containing (a) 0.0464 M $MgCl_2$ or (b) 0.0464 M $MgSO_4$. Both feed solutions also contained 0.232 mM LiCl, 0.232 mM KCl, and 0.232 mM CsCl. NF occurred at 6 bar through porous alumina membranes coated with a $(PSS/PAH)_4$ film. The crossflow rate was 26 mL/min.

half that for the other alkali ions, as reflected by the −40% rejection of Li^+ and the −200% rejection of K^+ and Cs^+.

When $MgSO_4$ is the dominant salt instead of $MgCl_2$, the rejection of Mg^{2+} decreases to 67%. This is consistent with the higher transference numbers of Mg^{2+} in $MgSO_4$ than in $MgCl_2$. The lower diffusion potential across the membrane with $MgSO_4$ relative to that with $MgCl_2$ also leads to less negative rejections of monovalent cations (compare Figures 8a and 8b). Nevertheless, the monovalent-ion negative rejections still follow the ion mobility trend, where LiCl has the smallest magnitude of negative rejection while CsCl has the most negative rejection.

CONCLUSIONS

PSS/PAH films show remarkable K^+/Mg^{2+} selectivities >350 in diffusion dialysis. However, the corresponding selectivity in nanofiltration is only 16, suggesting that convective transport of Mg^{2+} occurs (probably through membrane imperfections). Nevertheless, the extremely high dialysis selectivities might prove useful in electrodialysis, and we are investigating this possibility. Transmembrane electric potentials under concentration gradients show that PSS/PAH films are selectively permeable to anions, but this selectivity decreases with increasing salt concentrations. In nanofiltration, the differences in Mg^{2+} and Cl^- permeabilities give rise to electrical potentials across the membrane that lead to negative K^+ rejections as low as −200%. The magnitude of negative rejection increases with the trace ion mobility and might prove useful in selective removal of alkali cations from electrolyte mixtures containing multiply charged cations.

ASSOCIATED CONTENT

Supporting Information

Determination of transmembrane potentials; salt rejection based on the solution diffusion model; salt rejection with concentration polarization; possible contributions of concentration polarization to unexpectedly low Mg^{2+} rejections in nanofiltration; imperfections in nanoporous alumina supports. This material is available free of charge via the Internet at http://pubs.acs.org.

AUTHOR INFORMATION

Corresponding Author

*E-mail bruening@chemistry.msu.edu; Ph +1 517 355-9715 ext 237; Fax +1 517 353-1793.

Notes

The authors declare no competing financial interest.

ACKNOWLEDGMENTS

We gratefully acknowledge funding from the Division of Chemical Sciences, Geosciences, and Biosciences, Office of Basic Energy Sciences of the U.S. Department of Energy, through Grant DE-FG02-98ER14907.

REFERENCES

(1) Decher, G. Fuzzy Nanoassemblies: Toward Layered Polymeric Multicomposites. *Science* **1997**, *277*, 1232−1237.
(2) Decher, G.; Hong, J. D. Buildup of Ultrathin Multilayer Films by a Self-Assembly Process. 2. Consecutvie Adsoprtion of Anionic and Cationic Bipolar Amphiphiles and Polyelectrolytes on Charged Surfaces. *Ber. Bunsen-Ges.* **1991**, *95*, 1430−1434.
(3) Tagliazucchi, M.; Calvo, E. J. Charge Transport in Redox Polyelectrolyte Multilayer Films: The Dramatic Effects of Outmost Layer and Solution Ionic Strength. *ChemPhysChem* **2010**, *11*, 2957−2968.
(4) Adusumilli, M.; Bruening, M. L. Variation of Ion-Exchange Capacity, Zeta Potential, and Ion-Transport Selectivities with the Number of Layers in a Multilayer Polyelectrolyte Film. *Langmuir* **2009**, *25*, 7478−85.
(5) Bason, S.; Oren, Y.; Freger, V. Ion Transport in the Polyamide Layer of RO Membranes: Composite Membranes and Free-Standing Films. *J. Membr. Sci.* **2011**, *367*, 119−126.
(6) Bason, S.; Freger, V. Phenomenological Analysis of Transport of Mono- and Divalent Ions in Nanofiltration. *J. Membr. Sci.* **2010**, *360*, 389−396.
(7) Bason, S.; Kaufman, Y.; Freger, V. Analysis of Ion Transport in Nanofiltration Using Phenomenological Coefficients and Structural Characteristics. *J. Phys. Chem. B* **2010**, *114*, 3510−3517.
(8) Bason, S.; Kedem, O.; Freger, V. Determination of Concentration-Dependent Transport Coefficients in Nanofiltration: Experimental Evaluation of Coefficients. *J. Membr. Sci.* **2009**, *326*, 197−204.
(9) Bason, S.; Oren, Y.; Freger, V. Characterization of Ion Transport in Thin Films Using Electrochemical Impedance Spectroscopy II: Examination of the Polyamide Layer of RO Membranes. *J. Membr. Sci.* **2007**, *302*, 10−19.
(10) Toutianoush, A.; Schnepf, J.; El, H. A.; Tieke, B. Selective Ion Transport and Complexation in Layer-by-Layer Assemblies of p-Sulfonato-Calix[n]Arenes and Cationic Polyelectrolytes. *Adv. Funct. Mater.* **2005**, *15*, 700−708.
(11) Harris, J. J.; Stair, J. L.; Bruening, M. L. Layered Polyelectrolyte Films as Selective, Ultrathin Barriers for Anion Transport. *Chem. Mater.* **2000**, *12*, 1941−1946.
(12) Kim, B. Y.; Bruening, M. L. pH-Dependent Growth and Morphology of Multilayer Dendrimer/Poly(Acrylic Acid) Films. *Langmuir* **2002**, *19*, 94−99.
(13) Shiratori, S. S.; Rubner, M. F. pH-Dependent Thickness Behavior of Sequentially Adsorbed Layers of Weak Polyelectrolytes. *Macromolecules* **2000**, *33*, 4213−4219.
(14) Krasemann, L.; Tieke, B. Selective Ion Transport across Self-Assembled Alternating Multilayers of Cationic and Anionic Polyelectrolytes. *Langmuir* **2000**, *16*, 287−290.
(15) Krasemann, L.; Tieke, B. Composite Membranes with Ultrathin Separation Layer Prepared by Self-Assembly of Polyelectrolytes. *Mater. Sci. Eng., C* **1999**, *8*−*9*, 513−518.
(16) Krasemann, L.; Toutianoush, A.; Tieke, B. Self-Assembled Polyelectrolyte Multilayer Membranes with Highly Improved Pervaporation Separation of Ethanol/Water Mixtures. *J. Membr. Sci.* **2001**, *181*, 221−228.
(17) Krasemann, L.; Tieke, B. Ultrathin Self-Assembled Polyelectrolyte Membranes for Pervaporation. *J. Membr. Sci.* **1998**, *150*, 23−30.
(18) Meier-Haack, J.; Lenk, W.; Lehmann, D.; Lunkwitz, K. Pervaporation Separation of Water/Alcohol Mixtures Using Composite Membranes Based on Polyelectrolyte Multilayer Assemblies. *J. Membr. Sci.* **2001**, *184*, 233−243.

(19) Sullivan, D. M.; Bruening, M. L. Ultrathin, Gas-Selective Polyimide Membranes Prepared from Multilayer Polyelectrolyte Films. *Chem. Mater.* **2003**, *15*, 281−287.
(20) Leväsalmi, J. M.; McCarthy, T. J. Poly(4-Methyl-1-Pentene)-Supported Polyelectrolyte Multilayer Films: Preparation and Gas Permeability. *Macromolecules* **1997**, *30*, 1752−1757.
(21) Ouyang, L.; Malaisamy, R.; Bruening, M. L. Multilayer Polyelectrolyte Films as Nanofiltration Membranes for Separating Monovalent and Divalent Cations. *J. Membr. Sci.* **2008**, *310*, 76−84.
(22) Stanton, B. W.; Harris, J. J.; Miller, M. D.; Bruening, M. L. Ultrathin, Multilayered Polyelectrolyte Films as Nanofiltration Membranes. *Langmuir* **2003**, *19*, 7038−7042.
(23) Malaisamy, R.; Bruening, M. L. High-Flux Nanofiltration Membranes Prepared by Adsorption of Multilayer Polyelectrolyte Membranes on Polymeric Supports. *Langmuir* **2005**, *21*, 10587−10592.
(24) Miller, M. D.; Bruening, M. L. Controlling the Nanofiltration Properties of Multilayer Polyelectrolyte Membranes through Variation of Film Composition. *Langmuir* **2004**, *20*, 11545−11551.
(25) Saren, Q.; Qiu, C. Q.; Tang, C. Y. Y. Synthesis and Characterization of Novel Forward Osmosis Membranes Based on Layer-by-Layer Assembly. *Environ. Sci. Technol.* **2011**, *45*, 5201−5208.
(26) Qiu, C. Q.; Qi, S. R.; Tang, C. Y. Y. Synthesis of High Flux Forward Osmosis Membranes by Chemically Crosslinked Layer-by-Layer Polyelectrolytes. *J. Membr. Sci.* **2011**, *381*, 74−80.
(27) Setiawan, L.; Wang, R.; Li, K.; Fane, A. G. Fabrication of Novel Poly(Amide-Imide) Forward Osmosis Hollow Fiber Membranes with a Positively Charged Nanofiltration-Like Selective Layer. *J. Membr. Sci.* **2011**, *369*, 196−205.
(28) Qiu, C.; Setiawan, L.; Wang, R.; Tang, C. Y.; Fane, A. G. High Performance Flat Sheet Forward Osmosis Membrane with an NF-Like Selective Layer on a Woven Fabric Embedded Substrate. *Desalination* **2012**, *287*, 266−270.
(29) Wijmans, J. G.; Baker, R. W. The Solution-Diffusion Model - a Review. *J. Membr. Sci.* **1995**, *107*, 1−21.
(30) Baker, R. W. *Membrane Technology and Applications*; John Wiley & Sons, Ltd.: West Sussex, England, 2004.
(31) Bhanushali, D.; Kloos, S.; Bhattacharyya, D. Solute Transport in Solvent-Resistant Nanofiltration Membranes for Non-Aqueous Systems: Experimental Results and the Role of Solute-Solvent Coupling. *J. Membr. Sci.* **2002**, *208*, 343−359.
(32) Jin, W.; Toutianoush, A.; Tieke, B. Use of Polyelectrolyte Layer-by-Layer Assemblies as Nanofiltration and Reverse Osmosis Membranes. *Langmuir* **2003**, *19*, 2550−2553.
(33) Gilron, J.; Gara, N.; Kedem, O. Experimental Analysis of Negative Salt Rejection in Nanofiltration Membranes. *J. Membr. Sci.* **2001**, *185*, 223−236.
(34) Zhu, A.; Long, F.; Wang, X.; Zhu, W.; Ma, J. The Negative Rejection of H^+ in NF of Carbonate Solution and Its Influences on Membrane Performance. *Chemosphere* **2007**, *67*, 1558−1565.
(35) Yeo, S. J.; Kang, H.; Kim, Y. H.; Han, S.; Yoo, P. J. Layer-by-Layer Assembly of Polyelectrolyte Multilayers in Three-Dimensional Inverse Opal Structured Templates. *ACS Appl. Mater. Interfaces* **2012**, *4*, 2107−2115.
(36) Liu, X.; Bruening, M. L. Size-Selective Transport of Uncharged Solutes through Multilayer Polyelectrolyte Membranes. *Chem. Mater.* **2004**, *16*, 351−357.
(37) Amado, G. E.; Blanco, L. H. Osmotic and Activity Coefficients of Aqueous Solutions of KCl at Temperatures of 283.15, 288.15, 293.15 and 298.15 K- a New Isopiestic Apparatus. *Fluid Phase Equilib.* **2004**, *226*, 261−265.
(38) Pan, C. F. Osmotic and Activity Coefficients in Dilute Potassium Chloride Solutions at 25°C. *Can. J. Chem.* **1980**, *58*, 1386−7.
(39) Archer, D. G.; Wood, R. H. Chemical-Equilibrium Model Applied to Aqueous Magnesium-Sulfate Solutions. *J. Solution Chem.* **1985**, *14*, 757−780.
(40) Rodil, E.; Vera, J. H. Individual Activity Coefficients of Chloride Ions in Aqueous Solutions of $MgCl_2$, $CaCl_2$ and $BaCl_2$ at 298.2 K. *Fluid Phase Equilib.* **2001**, *187−188*, 15−27.
(41) Farhat, T. R.; Schlenoff, J. B. Doping-Controlled Ion Diffusion in Polyelectrolyte Multilayers: Mass Transport in Reluctant Exchangers. *J. Am. Chem. Soc.* **2003**, *125*, 4627−36.
(42) Stoykovich, M. P.; Daoulas, K. C.; Müller, M.; Kang, H.; de Pablo, J. J.; Nealey, P. F. Remediation of Line Edge Roughness in Chemical Nanopatterns by the Directed Assembly of Overlying Block Copolymer Films. *Macromolecules* **2010**, *43*, 2334−2342.
(43) Kielland, J. Individual Activity Coefficients of Ions in Aqueous Solutions. *J. Am. Chem. Soc.* **1937**, *59*, 1675−1678.
(44) Mulder, M. *Basic Principles of Membrane Technology*; Kluwer Academic Publishers: Dordrecht, Netherlands, 1996; pp 320−322.
(45) Bard, A. J.; Faulkner, L. R. *Electrochemical Methods: Fundamentals and Applications*; John Wiley & Sons: New York, 2000.
(46) Egueh, A.-N. D.; Lakard, B.; Fievet, P.; Lakard, S.; Buron, C. Charge Properties of Membranes Modified by Multilayer Polyelectrolyte Adsorption. *J. Colloid Interface Sci.* **2010**, *344*, 221−227.